IMAGE DENOISING BY MULTIPLE COMPRESSED SENSING RECONSTRUCTIONS

William Meiniel[1,2], *Yoann Le Montagner*[1,2], *Elsa Angelini*[2], *Jean-Christophe Olivo-Marin*[1]

[1]Institut Pasteur, Unité d'Analyse d'Images Biologiques, France
[2]Institut Telecom, Telecom ParisTech, CNRS LTCI, France

ABSTRACT

In this paper, compressed sensing (CS) is investigated as a denoising tool in bioimaging. Multiple reconstructions at low sampling rates are combined to generate high quality denoised images using total- variation sparsity constraints. The validity of the proposed method is first assessed on a synthetic image with a known ground truth and then applied to real biological images.

Index Terms— Bioimaging, compressed sensing, denoising, total-variation, Fourier transform.

1. INTRODUCTION

Image denoising consists in recovering an image x from a degraded noisy observation y. A deterministic denoising algorithm can then be viewed as a function g that maps the observation y to an estimator $\hat{x} = g(y)$ of x; g is designed to make $\hat{x}$ as faithful as possible to the ground truth x.

A very large number of image denoising methods exist in the literature, that consider different noise models and image characteristics (see [1]). Among them, total-variation based filtering [2] and non-local means (NLM) [3], and their variations, are at the basis of many current denoising approaches.

The use of total variation (TV) for denoising was originally proposed in [2]. and consists in obtaining the denoised estimator $\hat{x}$ as the minimum of the functional $\|x\|_{\mathrm{TV}} = \sum_{p,q} \sqrt{\partial_h x(p,q)^2 + \partial_v x(p,q)^2}$ where $\partial_h x$ and $\partial_v x$ are the partial horizontal and vertical derivatives of the image x, and p, q are the pixels of the image x. This method makes no assumption about the underlying nature of the noise. Optimization problems involving TV fit into the theory of convex optimization, which provides theoretical guaranties as well as efficient solvers to compute the denoising estimators (see [4], [5]). Moreover, it is well known that TV-based schemes tend to preserve the sharp edges present in the images and are therefore well adapted to biological microscopy images.

Inspired by the work of Marim et al. [6], we present a novel denoising method that exploits multiple redundant compressed sensing reconstructions while incorporating and taking advantage of total-variation based regularisation.

2. COMPRESSED SENSING AS A DENOISING TOOL

Compressed - or compressive - sensing (CS) is a sampling theory introduced in [7, 8], that states that if a discrete signal of size N is known to be sparse, it can be recovered from a set of M linear non-adaptive measurements, even if its size N is much larger than M. CS is robust to the presence of noise in the measurements, and can handle compressible signals (i.e. that are close from sparse signals for a certain norm). These latter extensions are important to deal with real-world data, for which noise-free images and perfect sparsity are often unrealistic hypothesis [9, 10].

2.1. Denoising by averaging of multiple CS reconstructions

The idea of our denoising method is based on the two following remarks. First, in terms of frequency analysis, the energy of a noise-free natural image is mostly concentrated in the low-frequency of its Fourier domain. Second, the theory of CS states that a sparse or compressible signal can be recovered from a non-adaptive subset of linear noisy measurements.

Based on these two facts, we propose to generate several correlated subsets considering the Fourier transform of the image, and rejecting most of its high frequency coefficients, which, as stated above, are corrupted. Each of these measurement subsets y_k $(k = 1, \ldots, R)$ is used to compute an estimator $\hat{x}_k$ of the ground truth image x through CS reconstruction. Finally, the $\hat{x}_k$ estimators are aggregated thanks to a fusion operator f, designed such that the resulting image $\hat{x} = f(\hat{x}_1, \ldots, \hat{x}_R)$ is less noisy.

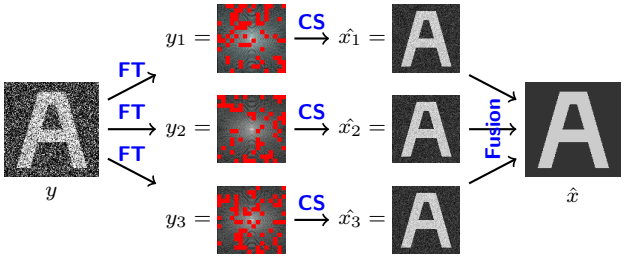

Fig. 1. **Denoising scheme using several CS reconstructions. From a noisy image y, we generate a given number of CS measurement vectors y_k, by taking the Fourier transform (FT) of y and selecting a subset of the Fourier coefficients, as presented in Fig. 2. Then, each y_k is used to produce an estimator $\hat{x}_k$ of the original signal through a CS reconstruction scheme. Finally, all the $\hat{x}_k$ are combined in a $\hat{x}$ estimator, with improved faithfulness properties.**

2.2. Implementation

The denoising method can be decomposed into three steps (see Fig. 1):

• *Generation of random subsets of measurement vectors y_k in the Fourier domain* : As mentioned above, each vector y_k is obtained through the selection of a different subset of Fourier coefficients of y. These selections are performed as the realization of a random selection process (see Fig. 2) designed as follows:

a. first, keep all the low-frequency coefficients below a certain cut-off spatial frequency ν_c,

b. second, sample in a uniform random manner the Fourier coefficients above ν_c, at a sampling rate $\tau \leq 1$.

We use different selection rules for low and high frequency coefficients to account for the properties mentioned in Sec. 2.1. The influence of the two parameters ν_c and τ is studied in Sec. 3. The generation of these measurement vectors can be written as a linear non-injective transformation: $y_k = \Phi_k y$, where Φ_k is constructed by rejecting several coefficients in a 2D Fourier transform matrix.

• *CS reconstructions generating partial estimators $\hat{x}_k$*: For each measurement vectors y_k, we resolve a CS reconstruction problem based on TV minimization, as proposed in [7]:

$$\hat{x}_k = \arg\min_x \|x\|_{\mathrm{TV}} \quad \text{s.t.} \quad \|\Phi_k x - y_k\|_2 \leq \epsilon \qquad (1)$$

with $\|\cdot\|_{\mathrm{TV}}$ defined as in [7]. The construction of Φ_k from a Fourier transform enables to solve (1) very efficiently using convex optimization algorithms [5].

• *Fusion of the $\hat{x}_k$ to produce a final denoised image $\hat{x}$*: To aggregate the series of partial estimators into a single scalar value per pixel, we define a fusion operator f as:

$$f(\hat{x}_1, \ldots, \hat{x}_R) = \frac{1}{R} \sum_{k=1}^{R} \hat{x}_k. \qquad (2)$$

We select f to be an averaging operator since the estimators are highly correlated and not noisy. This function verifies the basic property of being monotonic, which is important to preserve the original contrast in the image. It should be noted that if the $\hat{x}_k$ were R independent observations of the same signal, the energy of the residual noise in the fused image $\hat{x} = f(\hat{x}_1, \ldots, \hat{x}_R)$ would be divided by R compared to the noise in each $\hat{x}_k$. Even if in our case this hypothesis does not hold as the $\hat{x}_k$ are correlated, we still observe a reduction of the residual noise power in the fused image $\hat{x}$ (see Sec. 3).

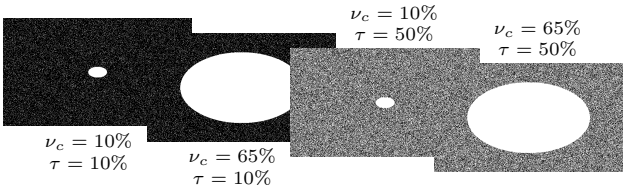

Fig. 2. **Examples of sampling masks used in the Fourier domain to generate the measurement vectors y_k. The white dots and areas correspond to the selected Fourier coefficients. See Sec. 2.2 for more details on the meaning of the parameters ν_c and τ.**

3. RESULTS

3.1. Dataset

One of the major problems when assessing the efficiency of denoising methods in biological imaging, is the lack of ground truth. A ground truth on a natural image cannot be found, and the use of classical noise-free images that we can find in the denoising literature does not correspond to our hypotheses.

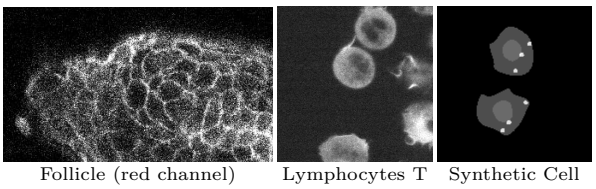

Fig. 3. **Natural and synthetic images used to assess the performances of our denoising algorithm.**

To quantitatively evaluate the quality of the proposed denoising method, we used a synthetic image generated by the SIMCEP simulator for fluorescent cell populations [11]. Simulated cells consist of nuclei, cytoplasm, and

intracellular objects. We used only the ground truth shape image, illustrated in 3 and corrupted with a mixed Poisson-Gaussian noise with parameters : $\sigma = 0.1$, $\lambda = 0.02$ (see Fig. 5).

In order to assess the quality of our method, we will use the Structural Similarity Index Measure (SSIM), a fidelity measure which takes into account the structural information in the image (see [12]).

To assess the performances of our denoising algorithm on real images, we used two sets of biological images (see Fig. 3): An image of fluorescently labelled T-lymphocytes, visualized with a confocal microscope, and the red channel of the fluorescently labelled image of hair follicle, visualized with a two-photon microscope.

3.2. Influence of the parameters

The proposed method uses three numerical parameters: ν_c and τ, that determine how the measurement vectors y_k are generated, and R, the number of intermediate fused CS reconstructions.

We first tested the influence of R on the SSIM: we noted that the SSIM increases exponentially with R, and that an almost optimal SSIM level is reached after a limited number of reconstructions only, whatever the parameters ν_c and τ (see [13]). The fact that only a small number of reconstructions is enough to converge is important for practical usage of the method, as the overall computation time of the method is proportional to R (the most expensive part of the method being indeed the successive CS reconstructions (1)). In the rest of the paper, we used $R = 10$.

We then tested the influence of the sampling parameters ν_c and τ on the final average image $\hat{x}$ (see Fig. 4). For low values of both parameters, the reconstructed images are of poor quality (upper left images in Fig. 4), while for high values, there seems to be no denoising (lower right images in Fig. 4): more precisely, using high values for τ and ν_c leads to estimators $\hat{x}$ for which the noise intensity remains significant in the parts of the images with objects present. Therefore we used intermediate values for τ and ν_c (50% and 25% respectively) in the rest of the paper.

3.3. Experience on a synthetic image

The proposed denoising algorithm was compared to NLM and TV-filtering. Results obtained on the synthetic cell image are presented on Fig. 5 where the denoised images are displayed along with the noise residues $|\hat{x} - y|$. These images show that the NLM method is unable to restore the weak contrast between the nuclei and the cytoplasm, and do not denoise the small intracellular structures at all. The TV-based method is corrupted with strong staircase artifacts. The proposed method performs better both visually and in terms of SSIM.

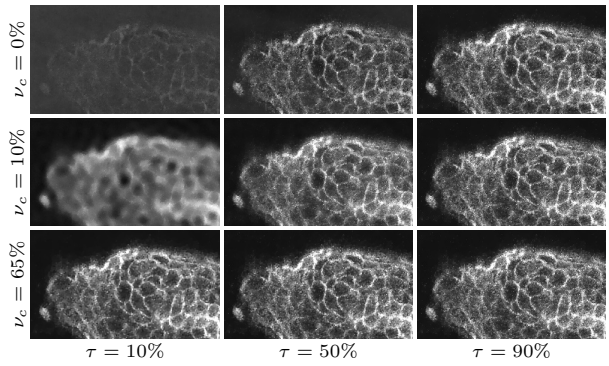

Fig. 4. **Denoising results via averaging of multiple CS reconstructions obtained on the hair follicle (red channel) image with different values of the sampling parameters ν_c and τ.**

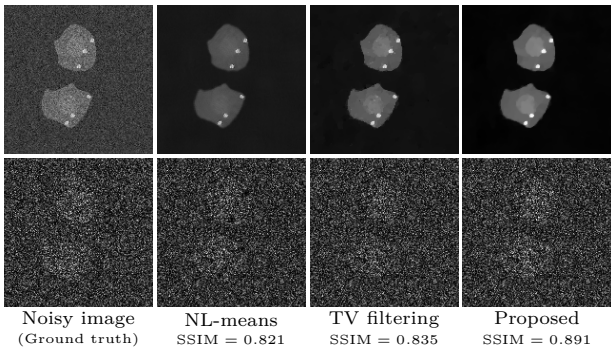

Fig. 5. **Denoising results on the synthetic cell image (perturbed with a mixed Poisson-Gaussian noise with parameters $\sigma = 0.1$ and $\lambda = 0.02$) obtained with the proposed algorithm and the standard methods. The top row presents the denoised images and the bottom row shows the corresponding noise residues. For the proposed algorithm, we used $R = 10$, $\nu_c = 25\%$, and $\tau = 50\%$. In this example, the ground truth is given, thus we can compute the SSIM of each reconstruction.**

3.4. Experience on biological images

Results obtained on the red channel of the hair follicle image and on the lymphocytes T image are respectively presented on Fig. 6 and 7. We cannot give quantitative results in terms of SSIM in this part because of the lack of a ground truth. However, the satisfying results on the synthetic image allow us to give qualitative comments about natural images.

We first notice that NLM performs poorly on these tested images, except in the background and in homogeneous areas, as can be seen in the residue maps. This

is probably due to the type of tested biological images, which present few non-random textured areas, and are therefore less favorable to the patch-search approach of NLM. Moreover, the residue map indicates that the NLM behavior highly depends on the local features in the images, thus leading to significant differences between areas in terms of denoising. It can also be seen that results achieved on the tested images with our method and TV-filtering present a much higher visual quality than with NLM. Finally, it can be observed that TV-filtered images are very similar to what is obtained with our proposed method when applied with high values of τ and ν_c.

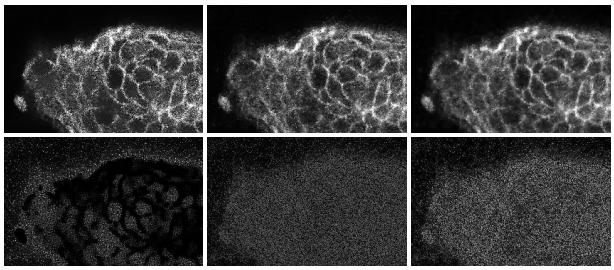

Fig. 6. **Denoising results on the hair follicle image (red channel) obtained with the proposed algorithm and the compared standard methods.**

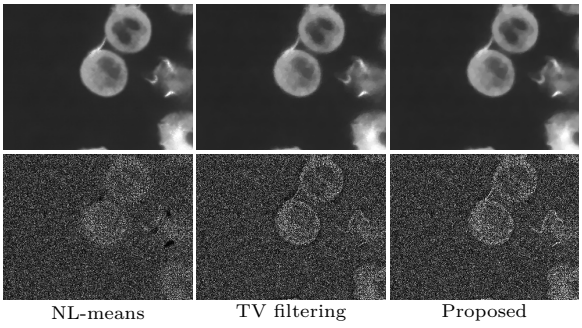

Fig. 7. **Denoising results on the lymphocytes T image obtained with the proposed algorithm and the compared standard methods..**

4. CONCLUSION

We have presented a new denoising method, that takes advantage of the CS framework with TV regularization. We have shown that this method achieves performances similar to standard denoising algorithms, while presenting more flexibility: one can adapt the parameters depending on each image that is processed.

This method bears as well the potential to combine acquisition and denoising once randomly programmable CCD cameras become readily available. We will address in future work the automated tuning of the optimal set of parameters for a given image.

Another promising development is the fusion step. Indeed, we can replace the mean fusion by any other mathematical operators. For instance, by computing the pixel-wise standard deviation of the R reconstructions, we obtain a so called variance map that shows where reconstruction errors are most likely to occur. Using this variance map to spatially adapt the fusion rule is the topic of ongoing research.

5. REFERENCES

[1] P. Milanfar, "A tour of modern image filtering: New insights and methods, both practical and theoretical," *Signal Processing Magazine*, vol. 30, no. 1, pp. 106–128, 2013.

[2] L. I. Rudin, S. Osher, and E. Fatemi, "Nonlinear total variation based noise removal algorithms," *Phys. D*, vol. 60, no. 1-4, pp. 259–268, 1992.

[3] A. Buades, B. Coll, and J-M. Morel, "A review of image denoising algorithms, with a new one," *Multiscale Modeling & Simulation*, vol. 4, no. 2, pp. 490–530, 2005.

[4] A. Chambolle, "An algorithm for total variation minimization and applications," *Journal of Mathematical imaging and vision*, vol. 20, no. 1-2, pp. 89–97, 2004.

[5] S. Becker, J. Bobin, and E. Candès, "Nesta: A fast and accurate first-order method for sparse recovery," *SIAM Journal on Imaging Sciences*, vol. 4, no. 1, pp. 1–39, 2011.

[6] E. Angelini M. Marim and J-C. Olivo-Marin, "Denoising in fluorescence microscopy using compressed sensing with multiple reconstructions and non-local merging," in *Int. Conference of the IEEE EMBS*, 2010.

[7] E. J. Candès, J. Romberg, and T. Tao, "Robust uncertainty principles: Exact signal reconstruction from highly incomplete frequency information," *IEEE Transactions on Information Theory*, vol. 52, no. 2, pp. 489–509, 2006.

[8] E. J Candès et al., "Compressive sampling," *Proceedings of the international congress of mathematicians*, vol. 3, pp. 1433–1452, 2006.

[9] M Marim, E. Angelini, J-C. Olivo-Marin, and M. Atlan, "Off-axis compressed holographic microscopy in low-light conditions," *Opt. Lett.*, vol. 36, no. 1, pp. 79–81, 2011.

[10] Y. Le Montagner, M. Marim, E. Angelini, and J-C. Olivo-Marin, "Numerical evaluation of sampling bounds for near-optimal reconstruction in compressed sensing," in *IEEE International Conference on Image Processing (ICIP)*, Sept 2011, pp. 3073–3076.

[11] P. Ruusuvuori et al., "Benchmark set of synthetic images for validating cell image analysis algorithms," in *16th European Signal Processing Conference*, August 2008.

[12] Z. Wang and AC. Bovik, "Mean squared error: Love it or leave it? a new look at signal fidelity measures," *IEEE Signal Processing Magazine*, vol. 26, no. 1, pp. 98–117, 2009.

[13] Y. LeMontagner, *Algorithmic solutions toward applications of compressed sensing for optical imaging*, Ph.D. thesis, Télécom ParisTech, 2013.